

Temperature-dependent shell effects in ^{16}O and ^{40}Ca with a realistic effective Hamiltonian

G. Bozzolo

*Physics Department, Case Western Reserve University, Cleveland, Ohio 44106
and Physics Department, Oberlin College, Oberlin, Ohio 44074*

O. Civitarese and J. P. Vary

W. K. Kellogg Radiation Laboratory, California Institute of Technology, Pasadena, California 91125

(Received 20 July 1987)

Finite temperature properties of ^{16}O and ^{40}Ca are evaluated self-consistently, with a realistic effective Hamiltonian. Resulting thermodynamic functions such as the free energy are analyzed to extract their smooth thermal dependence and the thermal dependence of the shell effects. The temperature dependence of single particle energies is large compared to results obtained with phenomenological Hamiltonians. Gaps between shell centroids decrease uniformly with increasing temperature. However, the spin-orbit splitting decreases even faster, so that the shell gap follows a pattern of an initial increase with temperature followed by an eventual decrease to zero at high T . This thermal blocking of the Hartree-Fock spin-orbit potential is associated with the thermal sensitivity of surface properties. The approximation of thermal occupation of the $T=0$ spectrum is also invalidated and the self-consistent treatment is necessary to obtain physical quantities such as the level density parameter as a function of T .

I. INTRODUCTION

The study of thermal excitations in finite nuclei has received much attention since there is great interest in nuclear properties far from the ground state.¹ A significant amount of work has been devoted both to schematic and realistic descriptions at finite temperature within Hartree-Fock,²⁻⁴ field treatments,⁵ and collective models.⁶⁻⁸

Recently, realistic effective Hamiltonians have been adapted to the finite temperature Hartree-Fock (FTHF) method.⁹ Hereinafter, we will address the role of finite temperature shell corrections in understanding the smooth and fluctuating contributions to the free energy surfaces.¹⁰⁻¹² We also address the consequences of self-consistency effects on the level density parameter.

Some of these temperature dependent effects have been investigated previously¹¹⁻¹² in a non-self-consistent scheme, namely, by assuming the constancy of single-particle energies over an extended temperature range. Although the collapse of shell corrections has been shown to occur, and a peak in the level density parameter has also been observed in the calculations,¹¹⁻¹² the question about the persistence of these results in a self-consistent treatment has not been answered yet. Within the present approach, the answer to this question is associated with the thermal sensitivity of surface related quantities.

We investigate this problem by performing calculations of shell corrections at finite temperatures within self-consistent finite temperature Hartree-Fock descriptions of ^{16}O and ^{40}Ca .

The formalism is briefly reviewed in Sec. II and the results are discussed in Sec. III. Some conclusions are drawn in Sec. IV.

II. FORMALISM

Here we shall briefly review some aspects of our realistic effective interaction. The details have been discussed previously.⁹ The effective Hamiltonian H_{eff} consists of three two-body operators each evaluated in a basis of harmonic oscillator states. First, there is the relative kinetic energy operator acting between all nucleon pairs. Second, we include a G matrix based on the Reid soft core interaction and the lowest order folded diagram for our no-core model space. Finally, the Coulomb interaction between protons is included. All the results reported here, unless specifically noted otherwise, are obtained with this H_{eff} evaluated for the lowest six major oscillator shells. The same model space was used extensively⁹ to evaluate some thermal properties of ^{16}O and ^{40}Ca .¹³ For the purposes of examining the role of larger model spaces, we add a phenomenological single-particle Hamiltonian acting on shells above the first six oscillator shells. This Hamiltonian consists of the single-particle kinetic energy operator, a Woods-Saxon potential of strength -60 MeV, diffuseness 0.6 fm, and radius $1.1A^{1/3}$ fm. In addition, to achieve a smooth matching with the HF spectrum at $T=0$, an additional overall positive shift of 20 MeV was added to the diagonal terms of the phenomenological Hamiltonian.

Following the notation of Ref. 9, we treat H_{eff} in the FTHF approximation, which is to minimize the free energy

$$F = H_{\text{eff}} - TS, \quad (1)$$

where T is the temperature and S is the single-particle entropy

$$S = - \sum_{\nu} [f_{\nu} \ln f_{\nu} + (1 - f_{\nu}) \ln(1 - f_{\nu})], \quad (2)$$

f_ν being the thermal occupation probabilities for fermions in orbitals labeled by ν , namely:

$$f_\nu = \left[1 + \exp \left(\frac{e_\nu - \mu}{T} \right) \right]^{-1}. \quad (3)$$

The chemical potentials μ are determined separately for neutrons and protons and e_ν are the self-consistent single-particle energies, which are the solutions of FTHF equations,

$$h | \nu \rangle = e_\nu | \nu \rangle, \quad (4)$$

with

$$\langle \alpha | h | \beta \rangle = \sum_\gamma \langle \alpha \gamma | H_{\text{eff}} | \beta \gamma \rangle f_\gamma. \quad (5)$$

In this context, we can write the FTHF energy as

$$\begin{aligned} E_{\text{HF}} &= \sum_\alpha e_\alpha f_\alpha - \frac{1}{2} \sum_{\alpha < \beta} \langle \alpha \beta | H_{\text{eff}} | \alpha \beta \rangle f_\alpha f_\beta \\ &= \frac{1}{2} \sum_\alpha e_\alpha f_\alpha. \end{aligned} \quad (6)$$

With this single-particle basis, we can calculate finite temperature shell corrections to the energy and free energy. The formalism has been presented in Ref. 12 and here we shall follow the same procedure. We can therefore introduce a smooth energy

$$\tilde{E} = \sum_\nu \int_{-\infty}^{\infty} de \tilde{g}_\nu(e) e f(e), \quad (7)$$

and a smooth entropy

$$\begin{aligned} \tilde{S} &= - \sum_\nu \int_{-\infty}^{\infty} de \tilde{g}_\nu(e) \{ f(e) \ln f(e) \\ &\quad + [1 - f(e)] \ln [1 - f(e)] \}, \end{aligned} \quad (8)$$

where¹²

$$\begin{aligned} \tilde{g}_\nu(e) &= \frac{1}{\gamma(\pi)^{1/2}} \exp \left[- \left(\frac{e - e_\nu}{\gamma} \right)^2 \right] \\ &\quad \times \sum_{m=0}^M a_{2m} H_{2m} \left[\frac{e - e_\nu}{\gamma} \right], \end{aligned} \quad (9)$$

is the smoothing function and $f(e)$ are the fermion occupation numbers defined as continuous functions of the energy e . Consequently, we can write for the smooth free energy the following expressions:

$$\tilde{F} = \tilde{E} - T\tilde{S}, \quad (10)$$

and we can relate this quantity with the FTHF free energy, namely¹²

$$F_{\text{HF}} = \tilde{F} + \delta\tilde{F}_{\text{shell}}. \quad (11)$$

Equation (11) is the finite temperature definition of the shell correction term $\delta\tilde{F}_{\text{shell}}$, in full analogy with the zero temperature case, where for the energy we have¹²

$$E_{\text{HF}} = \tilde{E} + \delta\tilde{E}_{\text{shell}}. \quad (12)$$

III. RESULTS AND DISCUSSION

The results for single particle energies, matrix elements of the effective interaction, and related global thermodynamical quantities have been presented in Ref. 9. We have repeated the calculations of Ref. 9 as well as new calculations in larger model spaces in order to obtain the single-particle bases which are needed for the present estimates of shell effects in ^{16}O and ^{40}Ca as a function of temperature. The most striking feature associated with temperature dependent effects, is the washing out of the spin-orbit splitting as shown in Fig. 1. Note that for both nuclei the spin-orbit splitting decreases by an amount between 30% and 50% as T increases from 0 to 6 MeV. The collapse of spin-orbit splittings occur for levels both above and below the Fermi energy. These results are in marked contrast with those obtained from the Skyrme Hamiltonian,^{2,6} where virtually no T dependence of the single-particle energies was reported in this temperature range.

A major consequence of this thermal blocking of the Hartree-Fock spin-orbit potential is that solutions show a change in the gap between major shells as illustrated in Fig. 2 for neutrons. The shell closure gap initially increases with T and eventually decreases. We note that

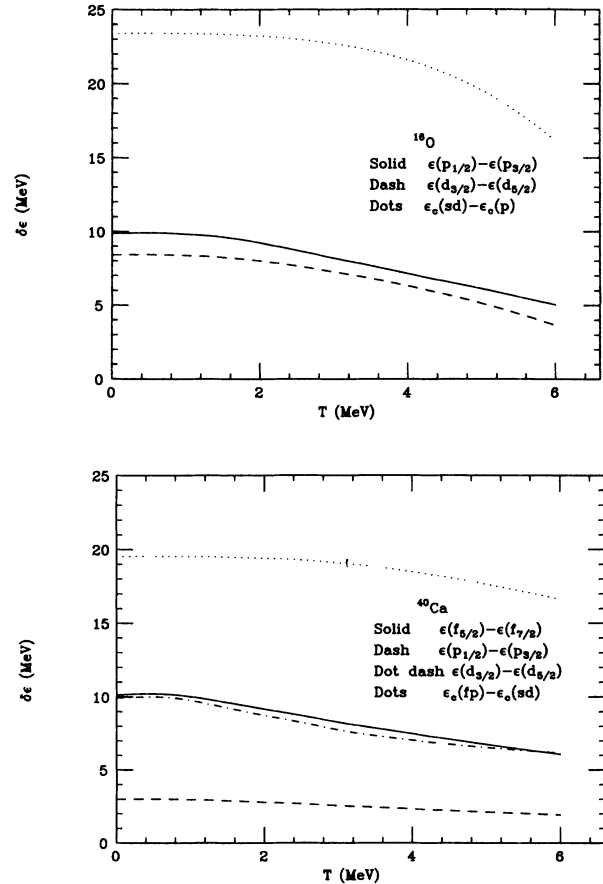


FIG. 1. Self-consistent spin-orbit splittings and gaps between shell centroids ϵ_c for ^{16}O and ^{40}Ca as a function of temperature T . All results are for the neutron single-particle energies.

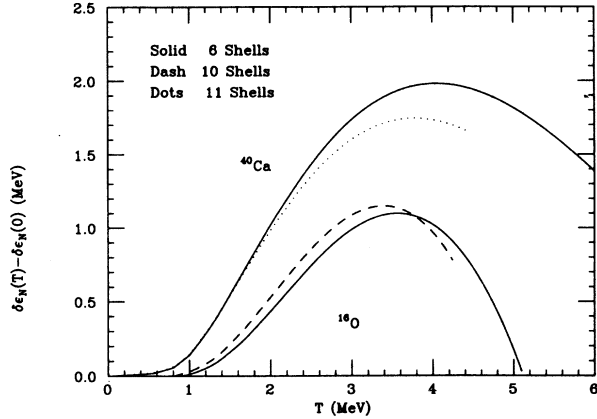


FIG. 2. Temperature dependence of the increase in the neutron shell gaps at the Fermi surface in ^{16}O and ^{40}Ca . Results are shown for radically different sizes of model spaces to assess the convergence. The two upper curves correspond to ^{40}Ca results while the two lower curves correspond to ^{16}O results.

this effect is well converged with our choice of model space as indicated in Fig. 2. Also, the increase in the gap is far more dramatic in ^{40}Ca than in ^{16}O . As a percentage of the $T=0$ gap, the increase is more than 20% in ^{40}Ca but less than 10% in ^{16}O . It will be interesting to observe in future work how large this increase becomes for heavier nuclei.

We present in Fig. 3 the results for the shell corrections to the free energy obtained with the procedures outlined in the previous section. In these calculations we have fixed the values of the smoothing parameter γ at $\gamma_{\text{neutrons}}=9.30$ MeV, $\gamma_{\text{protons}}=9.40$ MeV for ^{16}O , and $\gamma_{\text{neutrons}}=6.00$ MeV, $\gamma_{\text{protons}}=6.50$ MeV for ^{40}Ca .

The collapse of shell corrections, calculated for heavier systems and for a non-self-consistent single-particle level spacing,¹² appears to be confirmed by the present self-consistent results. It is remarkable that the critical temperature for the collapse of shell corrections (Fig. 3) corresponds closely with the temperature of the maximum increase in shell gaps (Fig. 2). The critical temperatures associated with the collapse of shell corrections can be

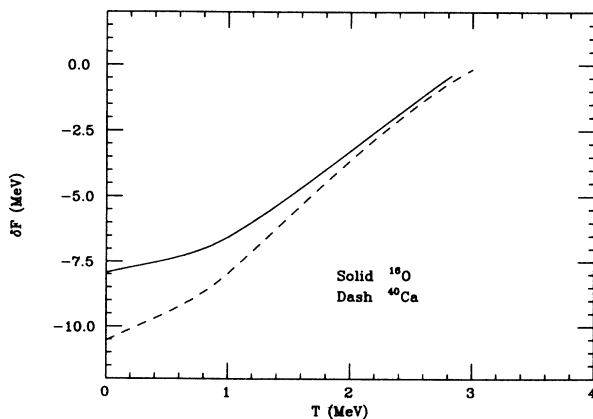


FIG. 3. Temperature dependence of the shell corrections to the free energy of ^{16}O and ^{40}Ca .

extracted from the values at zero temperature, namely¹² $(\delta\tilde{F}\rightarrow 0)_{T=T_c}$, where

$$T_c^{\text{shell}} = [-\delta\tilde{E}(T=0)/(\bar{a}-a_{\text{eff}})]^{1/2}, \quad (13)$$

and for the level density parameters \bar{a} and a_{eff} , corresponding to the smooth and effective free energies,¹² we have, respectively,

$$a_{\text{eff}} = -dF_{\text{HF}}^*/dT^2, \quad (14)$$

$$\bar{a} = (\pi^2/6)\bar{g}(\lambda_0).$$

With these values we have obtained, for ^{16}O , $T_c^{\text{shell}} \approx 2.9$ MeV, and for ^{40}Ca , $T_c^{\text{shell}} \approx 3.1$ MeV.

Let us now discuss the behavior of the level density parameter as a function of temperature.² The currently adopted description of this behavior, which is mainly based on the assumption of a constant, almost T -independent, single-particle spectra, shows a strong temperature dependence at low temperatures.^{6,11}

The results for E_{HF} as a function of T from our self-consistent approach are shown in Fig. 4 along with mean excitation energies evaluated with the single-particle solutions of the HF equations at zero temperature. We refer to the latter results as finite temperature shell model (FTSM) results. The difference between estimates of the

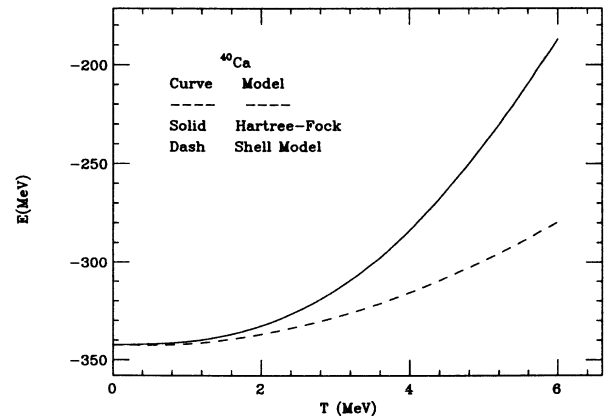
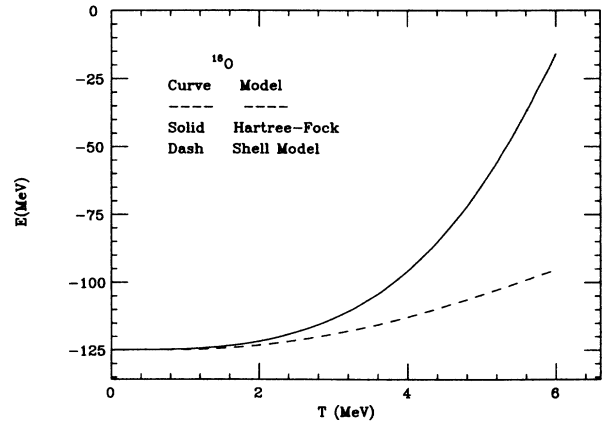


FIG. 4. Temperature dependence of the FTHF energy ("Hartree-Fock") and of the energy obtained by thermally occupying the HF ($T=0$) spectrum ("shell model").

excitation energy is approximately a factor of 2 over the range of T shown.

The different slopes arising for $E(T)$ are particularly significant for calculations of the level density parameter $a(T) = dE/dT^2$. The results are shown in Fig. 5. The values of $a(T)$ for the FTHF results differ strongly from the FTSM values which indicates self-consistency effects are large. It should be noted that when the temperature dependence is accounted for only by the occupation numbers, $f_\nu(\epsilon_\nu(T=0))$, the level density parameter displays a peak. In this context, and for temperature independent single-particle energies, the appearance of a peak in $a(T)$ is a consequence of the structure of the corresponding characteristic determinant which defines the denominator of the level density formula,¹¹ namely

$$D(T) \approx \sum_i f_\nu(\epsilon_\nu(0)) [1 - f_\nu(\epsilon_\nu(0))], \quad (15)$$

which clearly reaches an extreme value for levels nearby the Fermi one. This peaking behavior does not manifest itself in the case of the self-consistent FTHF calculations, where both the single-particle energies and the occupation numbers are temperature dependent. The reason is that Eq. (15) for $D(T)$, when evaluated in FTHF, displays a larger width than the $D(T)$ for FTSM. The

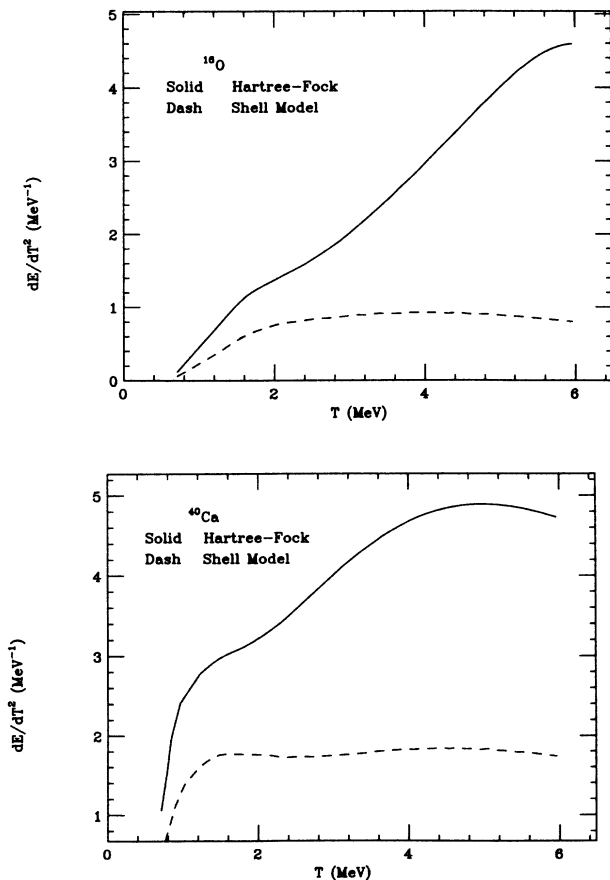


FIG. 5. Temperature dependence of the level density parameter dE/dT^2 evaluated from the FTHF results ("Hartree-Fock") and from the energy obtained by thermally occupying the HF ($T=0$) spectrum ("shell model").

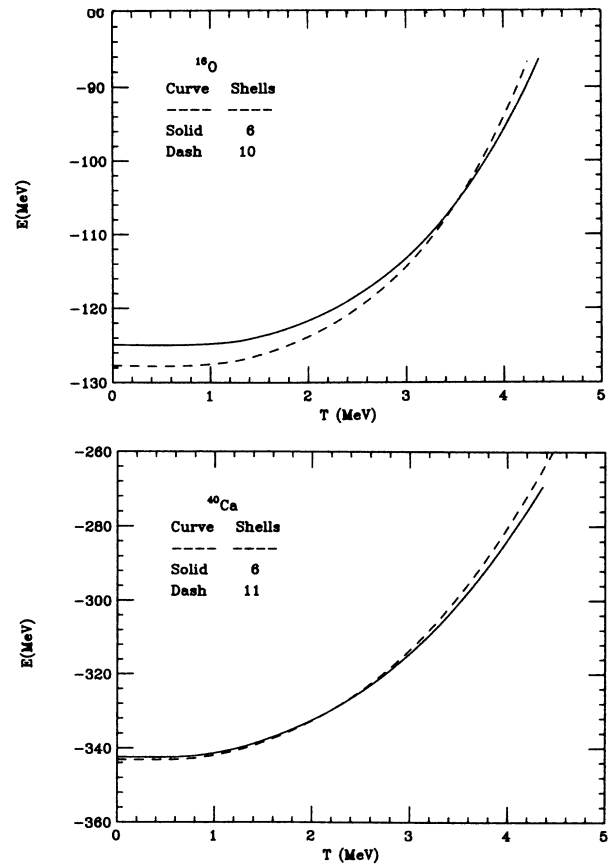


FIG. 6. Energy in the FTHF approximation as a function of T^2 for two choices of oscillator model spaces—six shells and ten shells (^{16}O) or eleven shells (^{40}Ca). For the ^{40}Ca results in six-shells only shown here, we have used the parameters $(\lambda_1, \lambda_2, \hbar\omega) = (0.985, 1.29, 7.87 \text{ MeV})$ since they yield approximately the same ground state ($T=0$) binding and rms radius as the eleven-shell results with $(\lambda_1, \lambda_2, \hbar\omega) = (1.00, 1.29, 7.61 \text{ MeV})$. The latter parameter values are used for all other six-shell results in this work.

larger width results in a non-peak structure for $a(T)$. Nevertheless, $a(T)$ is a strongly T -dependent function, a feature which does not emerge from the studies of semi-infinite or infinite media at finite temperature.¹⁴

Our results for ^{40}Ca differ in several respects from those reported in Ref. 6 where a phenomenological Hamiltonian was employed. The magnitude of our level density parameter obtained from the self-consistent results is approximately the same as that of Ref. 6 even though the results of Ref. 6 were obtained with a single-particle spectrum which was independent of temperature. The resolution of this apparent paradox lies in the fact that the shell gap in Ref. 6 in ^{40}Ca ($d_{3/2}$ to $f_{7/2}$ splitting) is only about 4 MeV which is less than one-half of our shell gap of 9.3 MeV. The smaller gap facilitates thermal excitations and augments the level density parameter which explains the difference of the results in Ref. 6 from our FTSM results shown in Fig. 5.

IV. CONCLUSIONS

In this paper we have reported some results concerning the temperature dependence of shell effects in ^{16}O and

⁴⁰Ca. We have used in our calculations an effective realistic Hamiltonian, treated within the FTHF approximation. The temperature dependence of the self-consistent HF solutions has a significant effect on the behavior of the level density parameter $a(T)$. We have found that the temperature dependence of the single-particle spectrum is large and induces a change of more than a factor of 2 in $a(T)$ at temperatures below 6 MeV. This effect could be important for estimating critical temperatures associated with compound nucleus decay channels at finite temperatures.¹⁵ Further investigations are in progress concerning this problem.¹⁶

ACKNOWLEDGMENTS

One of us (G.B.) acknowledges partial support from Oberlin College under the Affiliate Scholar Program. O.C. is a fellow of the National Research Council of Argentina and a staff member of the Department of Physics of the University of La Plata, Argentina. This work was supported in part by the National Science Foundation Grant Nos. PHY85-05682, PHY86-04197, and INT84-13827, and by the U.S. Department of Energy under Contract Nos. DE-AC02-82ER40068, DE-AC02-85ER40199, and Grant No. DE-FG02-87ER40371, Division of High Energy and Nuclear Physics.

¹M. Lefort, Nucl. Phys. **A387**, 3C (1982).

²M. Brack and P. Quentin, Nucl. Phys. **A361**, 35 (1981).

³A. L. Goodman, Nucl. Phys. **A352**, 30 (1981); **A352**, 45 (1981); **A369**, 365 (1981); **A370**, 90 (1981); **A402**, 189 (1983).

⁴A. L. Goodman, Phys. Rev. C **29**, 1887 (1984).

⁵A. K. Kerman, S. Levit, and T. Troudet, Ann. Phys. **148**, 436 (1983).

⁶W. Besold, P.-G. Reinhard, and C. Toepffer, Nucl. Phys. **A431**, 1 (1985).

⁷N. Vinh Mau and D. Vautherin, Nucl. Phys. **A445**, 245 (1985).

⁸P. Bonche, S. Levit, and D. Vautherin, Nucl. Phys. **A427**, 278 (1984).

⁹G. Bozzolo and J. P. Vary, Phys. Rev. C **31**, 1909 (1985).

¹⁰Y. Alhassid and J. Zingman, Phys. Rev. C **30**, 684 (1984).

¹¹O. Civitarese and A. L. De Paoli, Nucl. Phys. **A440**, 480 (1985).

¹²O. Civitarese *et al.*, Z. Phys. A **305**, 341 (1982); **309**, 177 (1982); **311**, 317 (1983).

¹³In the notation of Ref. 9 the parameters $\lambda_1, \lambda_2, \hbar\omega$ chosen for ¹⁶O(⁴⁰Ca) were 0.977, 1.35, 8.65 (1.00, 1.24, 7.61), in order to approximate the correct $T=0$ binding energy and rms radius. The binding energy obtained is -124.9 (-320.7) MeV and the point rms radius obtained is 2.62 (3.48) fm for calculations in six major shells. These parameters differ slightly from those of Ref. 9 and result from fits to the ground state properties in larger model spaces. We have checked that none of the results reported in Ref. 9 is significantly changed.

¹⁴J. Bartel, M. Brack, C. Guet, and H.-B. Håkansson, Phys. Lett. **139B**, 1 (1984).

¹⁵G. La Rana *et al.*, Phys. Rev. C **35**, 373 (1987).

¹⁶G. Bozzolo, O. Civitarese, and J. P. Vary, Phys. Rev. C (in press).